By acceptance of this article, the publisher or recipient acknowledges the U.S. Government's right to retain a nonexclusive, royalty-free license in and to any copyright covering the article.

CONF-830590--2

Electron-Cyclotron-Heating Experiments in Tokamaks and Stellarators*

A. C. England

Fusion Energy Division

Oak Ridge National Laboratory

Oak Ridge, Tennessee 37830

CONF-830590--2

DE83 017210

Abstract

This paper reviews the application of high-frequency microwave radiation to plasma heating near the electron-cyclotron frequency in tokamaks and stellarators. Successful plasma heating by microwave power has been demonstrated in numerous experiments. Predicted future technological developments and current theoretical understanding suggest that a vigorous program in plasma heating will continue to yield promising results.

INTRODUCTION

The major disadvantage of this technique has been the lack of high-frequency sources. This disadvantage is gradually disappearing with the development of high power gyrotrons. Another disadvantage is that the technique heats electrons only. However, at high densities

*Research sponsored by the Office of Fusion Energy, U.S. Department of Energy, under contract W-7405-eng-26 with the Union Carbide Corporation

MASTER

DISTRIBUTION OF THIS DOCUMENT IS UNLIMITED

the coupling between ions and electrons will be good enough that they will reach the same temperature. In addition, there is a density limit and (provided that the temperature is limited) a concomitant beta limit. However, this limit is not serious for high-frequency sources at high magnetic fields. Another disadvantage for contemporary devices is that high-field launch is best; however, for very large future devices this high-field launch may not be preferred over low-field launch. Low field launch represents a distinct engineering advantage.

One advantage of heating with high-frequency microwaves that the process is localized, allowing energy to be deposited in narrow regions. Another is that the process is very efficient for carefully controlled launching, so that all the energy can be absorbed where it is needed. Furthermore, the antennas are generally small in comparison to the antennas in other frequency ranges, and there is no problem with coupling. In present-day devices and in devices now contemplated for the near future, no matching elements are generally needed.

Electron cyclotron resonance heating, here termed electron cyclotron heating or ECH for convenience, has been described in a large body of literature. For the process to occur, there must be power (i.e., an electric field) at the electron cyclotron frequency in a magnetic field in an evacuated chamber with some low gas density. Although the process has been known and used for many years in fundamental plasma physics studies, the first important use of ECH for plasma heating was in small mirror machines.[1]

The process has become important with the development of high-power short-wavelength microwave sources. In particular, the development of the gyrotron has given great impetus to this line of research. Although a number of groups were involved in the early development of the gyrotron,[2] the early exploitation of the gyrotron concept in the U.S.S.R.[3] permitted Soviet physicists to quickly determine that ECH was an important heating technique in tokamaks. Since that time, the early lead that the Soviets achieved in gyrotron development has allowed them to maintain their superiority in this area. Only recently have developments in the West permitted gyrotrons to approach the frequency and power levels achieved in the U.S.S.R.

There are actually several applications for ECH. The most commonly considered application is bulk heating. However, there is some evidence for current drive, and several experiments are now exploring that possibility. Another important area is profile modification and the associated magnetohydrodynamic (MHD) instability suppression. Preionization and start-up have been shown to be useful in tokamaks, and prospects for the use of ECH in these applications look encouraging. It appears that ECH can be profitably used as an adjunct to other heating techniques. It could be used for independent control of electron temperature T_e or for current profile control with ion cyclotron heating or neutral beam injection.

Elementary Theory

The Clemmow-Mullaly-Allis (CMA) diagram for cold electron plasma is shown in Fig. 1. The solid horizontal line at $\omega_{ce}^2/\omega^2 = 1$ represents the cyclotron resonance; the line marked upper hybrid represents the upper hybrid resonance $\omega_{pe}^2 + \omega_{ce}^2 = \omega^2$; and the line marked "cut off" between regions 1 and 4 represents the right-hand cutoff boundary for the extraordinary wave and is defined by

$$\omega_R = \frac{\omega_{ce}}{2} + [(\frac{\omega_{ce}}{2})^2 + \omega^2_{pe}]^2/2.$$

At a resonance the index of refraction n goes to infinity ($n \to \infty$) and at a cutoff, such as ω_R, $\underline{n} = 0$. The solid arrow shows an optimum path of radiation incident from the inside of a tokamak, where the magnetic field is large and $\omega_{ce} > \omega$.

The extraordinary wave is cut off in region 4. If a wave is launched from the low-field side [i.e., $(\omega_{ce}/\omega)^2 < 1$], it will encounter the cutoff ω_R. The right-hand wave is absorbed at cyclotron resonance in regions 5 and 8. The left-hand wave can propagate in regions 3 and 6, but no wave can propagate in region 7. The boundary between regions 6 and 7 is due to the left-hand cutoff,

$$\omega_L = -\frac{\omega_{ce}}{2} + [(\frac{\omega_{ce}}{2})^2 + \omega_{pe}^2]^{1/2}.$$

In high-density cases the plasma center is cut off to the extraordinary

wave by this resonance ω_L. Such densities are typical of today's high-beta tokamak operation.

Heating at the second harmonic [$(\omega_{ce}/\omega)^2 = 0.25$ on the ordinate of Fig. 1] is possible without encountering the right-hand cutoff if the density is not too large [$(\omega_{pe}/\omega)^2 < 0.5$]. Second harmonic heating has been shown to be effective in high-temperature plasmas. The absorption process involves finite orbit effects.

To further clarify the points about fundamental heating, Fig. 2 illustrates the regions of propagation and evanescence for a typical tokamak with the resonance located at the center of the plasma chamber. Projected on the cross section are the cutoffs, resonances, and evanescent regions for (a) a low-density, (b) a moderate-density, and (c) a high-density plasma for the extraordinary wave propagation. Note that the ECH and UH regions are always accessible from the high-field side, but in the highest-density cases the plasma center is shielded by the left-hand cutoff ω_L. The highest-density case is typical of contemporary tokamak operation with high beta. Such densities are generally too high for ECH because of the cutoffs, and densities more typical of Fig. 2b are generally used.

In contrast, if the ordinary wave is used, there is no UH resonance and the only cutoff is at ω_{pe}. This cutoff at the critical density n_c is illustrated in Fig. 2 by a dotted line. The O-mode critical density is typically ~1/2 that of the extraordinary mode. In the cold plasma theory, collisional damping of this wave is possible;

in the hot plasma theory, there is cyclotron damping, which is maximum for propagation normal to the confining magnetic field.

Early Experiments in the USSR

Significant early experiments on ECH were performed in tokamaks at two laboratories in the U.S.S.R. As early as 1971, both Alikaev at the Kurchatov Institute in Moscow and Golant at the Ioffe Institute in Leningrad had performed high-power experiments.

Golant[4] used a microwave source of 80 kW at 9 GHz on the TUMAN-2 tokamak for fundamental ECH studies at low (~ 5-kG) magnetic fields. Pulse lengths were between 100 and 300 μs. Also, 100-μs pulses of 30 kW at 34 GHz were used for second harmonic ECH. At 9 GHz, the heating was thought to be due to wave conversion at the UH layer. The presence of a cyclotron resonance layer was necessary for heating, and the heating efficiency was correlated with the position of the evanescent region and the magnitude of the conversion efficiency.[5] A heating efficiency of 60% could be obtained under optimum conditions.

For second harmonic heating, the energy change in the plasma could not be measured directly but could be inferred from the change in the plasma current.

Based on this, the heating efficiency was estimated to be 5-10%; the low value was attributed to larger attenuation in the evanescent region and lower conversion efficiency.

Alikaev[6] used ~40 kW of microwave power at ~30 GHz for 500 μs in the TM-3 tokamak. In a cold plasma, he found no heating at the second harmonic, but found heating both with and without a fundamental cyclotron resonance. This was attributed to the UH resonance and collisional heating. In hot plasmas (T_e > 200 eV), absorption at the second harmonic was observed. The efficiency of heating at the fundamental was given as 20-30%.

In 1972,[7] Alikaev et al. reported further measurements with a 30-GHz time microwave source on TM-3. An increase of the energy containment time τ_E with T_e was observed, as were damping of oscillations during the microwave pulse, a decrease in the high-energy (>10-keV) x-ray intensity, a shift of the plasma column outward, and a decrease in the loop voltage. Some of these effects could be attributed to bulk heating.

In 1973 Golant et al.[8] reported experiments in the FT-1 tokamak (Fig. 3). Sources supplying 50 kW at 30 GHz and 12 kW at 22 GHz were used, both with pulse times of 200 μs. Fundamental cyclotron heating was observed at 22 GHz with an absorption efficiency of 30%. Because of the low temperature, some absorption could be attributed to collisions. The efficiency of absorption could be qualitatively related to the thickness of the evanescent regions and the location of

the UH surface. Effects of second harmonic absorption at 30 GHz could be observed over a very narrow region (~4 cm thick), and the efficiency of the absorption was not high.[9]

The absorption process at 22 GHz was attributed to linear wave transformation of the microwave energy at the UH surface. The plasma waves arising from this transformation were believed to be absorbed between the UH and cyclotron resonance surfaces.

In 1974 Alikaev et al.[10] reported further measurements on TM-3 using 30 GHz with up to 70 kW of power and a pulse length of 1 ms. Runaway electrons were observed by the bremsstrahlung radiation and by millimeter microwave radiation when the axial magnetic field was higher than the resonant magnetic field by 30%; that is, when the resonance zone was displaced to the outside. The x-ray measurements suggested that electrons with a longitudinal energy of ~20 keV did not acquire more than 10% of the plasma energy gain measured diamagnetically. The number of runaway electrons could be minimized by operating at high density. Also, applying the microwave power early did not increase the runaway population.

With the magnetic field adjusted for electron cyclotron resonance on axis, the number of runaways was decreased. In operations with the resonance on axis, the measurements suggested that only 25% of the bulk of the electrons was heated. In any case, no ion temperature increase was observed.

Following this, Alikaev et al.[11,12] reported further measurements on TM-3. Laser Thomson scattering was used to measure the central electron temperature (Fig. 4). Measurements made with the resonance field on axis showed bulk heating of the plasma at both the fundamental and the second harmonic, but experiments at the second harmonic caused some runaway production. Also, heating at the second harmonic resulted in an increase in poloidal beta β_p to 2.2. The lifetime of the runaways was estimated at 2 ms for 10-keV electrons and 9 ms for 60-keV electrons. The energy containment time τ_E was found to be proportional to the electron temperature T_e (Fig. 5) and the thermal conductivity κ_e was inversely proportional to T_e. These results may have been fortuitous, as later experiments on T-10 (described below) did not support this conclusion.

A later analysis of the TM-3 experiments by Poznyak[13] concluded that the resistive losses in the chamber walls were very important in a small device such as TM-3. The absorption characteristics for the first and second harmonics were comparable. The absorption of the second harmonic was limited to 40-60% of the input power by the wall absorption; actually, plasma absorption did not exceed 10-20% for linear processes. The absorption was linear with power within 20% up to power levels of 100 kW.

The absorption of the fundamental and second harmonic was shifted toward the periphery of the plasma at high density, but actual absorption near the surface was weak. There appeared to be little

absorption at the UH resonance. It also appeared that the main characteristics of the absorption could be explained without recourse to absorption by runaways, but this possibility could not be entirely ruled out.

All of the experiments in the U.S.S.R. were made with the microwave feed on the outside (low-field side) of the torus. Hence, there is the possibility that the evanescent region on the low-field side interfered with the extraordinary wave propagation. Since in many of the experiments the guide was circular, the actual wave launched could be a combination of ordinary and extraordinary polarized radiation. In the last experiment on TM-3, a horn was used, primarily to launch the ordinary wave. In later experiments, gyrotrons were used to supply the microwave power. There is no evidence in the published literature that any kind of a matching device other than a horn was used. It should be noted also that in almost all cases, overmoded circular guides were used.

To summarize this section briefly, these early experiments showed that ECH was a good technique for bulk plasma heating and provided an impetus to extrapolate the technology to higher power and higher frequency as well as to explore high-field launching.

First Experiments Outside the U.S.S.R.

The first experiment in the United States by Gilgenbach et al.[14] on the Impurity Study Experiment (ISX-B), showed strong heating. It utilized a 35-GHz gyrotron built at the Naval Research Laboratory (NRL) with a pulse length of up to 16 ms and a power of 80 kW delivered to the tokamak. A high-field side (inside) antenna was used, but the radiation was unpolarized. As in the U.S.S.R. experiments, an overmoded circular guide was used. The window was located so that the cyclotron resonance was in the pressurized guide (Fig. 6). A central temperature rise of ~400 eV was observed but with a line-averaged density drop of about 15% (see Fig. 7). The heating was found to be linear with power with 5.5 eV/kW measured; the average density was 1.0 $\times 10^{13}$ cm^{-3}. About 60% efficiency was reported, which was comparable to theoretical calculations (<75%). The measured temperature rise was in good agreement with a transport code that used an empirical heat conduction coefficient independent of T_e. No ion heating was observed and none was expected due to the low density. Later experiments by the same group[15] showed the advantages of preionization by ECH. A reduction in the initial loop voltage of 40% was achieved, flux (volt-second) savings in the transformer were observed, and a more rapid current rise was achieved. There was evidence that the power was deposited first in the cyclotron resonance layer and later in the UH layer. High electron temperatures (~50 eV) were observed there.

On TOSCA in the United Kingdom,[16-18] heating at the second harmonic was successfully achieved with a 28 GHz gyrotron. A power level of up to 150 kW and pulse lengths of up to 3 ms were used. The unpolarized radiation was injected from the outside. The loop voltage

dropped by as much as 50%, and the plasma energy (measured diamagnetically) increased. Heating was observed at densities above the extraordinary mode (X-mode) cutoff. Poloidal beta values of ~4 (approximately equal to the aspect ratio) were achieved, and a nonlinear dependence of the stored energy on the ECH power was observed. Soft x-ray emission indicated the presence of strong local heating near the cyclotron resonance. A sustained temperature maximum observed on one side of the magnetic axis maximum observed (see Fig. 8) could be accounted for by reducing the parallel heat conduction coefficient by a factor of 100 or by invoking trapped electrons. There was some evidence of current drive, but the effect was not large. Radiation was directed with and against the toroidal current by a rotating quartz prism. Strong losses (25%) in the prism existed but were acceptable for the short pulse lengths used. The small current-drive effect was attributed to the low single-pass absorption and to the presence of trapped electrons.[18]

In a related experiment,[19] which is not actually within the scope of this paper, current drive by ECH was observed on the Culham Levitron. With a 10-GHz microwave source of 120 W, currents of 30 mA/W were observed. The current scaled according to theory, but the actual magnitude was larger than expected.

Another 28 GHz gyrotron was taken to Japan for an experiment on JFT-2. Both outside[20] and inside[21] launches were used with pulse lengths of up to 16 ms. For the outside launch (see Fig. 9) [ordinary mode (O-mode)], an electron temperature rise of more than 500 eV was

observed with 114 kW of power for a 14 ms pulse. There were loop voltage reductions of 30% and a density decrease of up to 15%. Central heating was observed with densities up to $1.0n_c$. Heating off axis was observed for central toroidal fields above and below that needed for central heating. The launching system used eight small horns launching O-mode power slightly (~10o) off normal to the field.

The inside launch experiments used a phased antenna array that could be externally directed over a range from 42o to 60o from the normal (i.e., the parallel index of refraction was: $0.66 < n_{\parallel} < 0.86$) (see Fig. 10). An eight-arm mode converter converted the TE_{02} waveguide mode power from a large overmoded circular guide to the TE_{10} mode in eight fundamental mode waveguides feeding the antenna. The 200 kW gyrotron pulse lasting 15 ms was reduced in power by mode conversion and transmission losses to typically 80-85 kW. The central temperature could be doubled (from 600 eV to 1200 eV) with ECH power of two-thirds of the ohmic input. Oblique launching showed much better heating than either normal inside launching, or the outside launching mentioned earlier (see Fig. 11). Heating was observed up to the critical density.

The same gyrotron used on ISX-B was later installed on the VERSATOR[22] tokamak at the Massachusetts Institute of Technology (MIT). A rotating antenna was used to direct the polarized radiation upfield and downfield for current-drive investigations (see Fig. 12). Loop voltage reductions of 60% were reported, and there is some possibility that current drive was achieved. However, since the single-pass

absorption was weak, current-drive theories would predict a very small effect. Decay radiation from a three-wave coupling process was observed.[23] The observations are consistent with extraordinary wave coupling at the UH layer to a lower hybrid (LH) wave and an electron Bernstein mode. The fact that low single-pass absorption occurred meant that sufficient power reached the UH layer to cause this mode coupling.

In Japan, two small experiments have achieved excellent results with ECH. The WT-I tokamak[24] used a 16-GHz gyrotron with an output power of 2.5 kW for 1 ms. Preionization was successful, but bulk heating was not attempted. The WT-II tokamak[25] used a 22-GHz gyrotron with a 25-kW output power to launch a mixed mode into the outside of the vacuum vessel. Because of the small size of the experiment, diagnostics could not demonstrate bulk heating, but there was a reduction of the loop voltage.

Later Experiments in the U.S.S.R.

Experiments on the large tokamak T-10 commenced in 1979 with two 200-kW gyrotrons at ~85 GHz (~3.6-mm wavelength).[26] By 1980,[27] four gyrotrons were in place, each with a power output of 200-kW and a maximum pulse length of 150 ms. The gyrotron complex has been further described by Flyagin.[28] For these experiments, the magnetic field was reduced so that only second harmonic heating could be attempted. (This was due to a problem with the toroidal field power supply and was not

related to the ECH experiment.) The power was fed to the plasma from the outside through four overmoded waveguides (each 8 cm in diameter) aimed at the center of the plasma, as shown in Fig. 13, to minimize refractive effects. About 70% of the output power was in the O-mode. Whereas only 30% of the ordinary O-mode was expected to be absorbed, measurements showed that 90% was absorbed. The extraordinary wave was completely absorbed within the accuracy of the measurement. The energy containment time was found to be unaffected by the heating. There was some increase in impurity imput during ECH, but the radiation losses increased less than 10%. There was a density decrease during ECH and also a small ion temperature rise.

Further experiments were reported in 1982 by Alikaev et al.[29] in which up to 500 kW of power from this gyrotron complex was produced for pulse lengths of up to 60 ms. Fundamental ECH was employed with the full toroidal field of 30 kG. There were two types of discharges and two regimes of operation: (1) At a density of 2.8×10^{13} cm^{-3} and an initial $T_e(0)$ of 1.5 keV, a temperature rise of 0.9 to 1.0 keV was observed. The heating efficiency was found to be 64% in this case. Again, the density decreased and there was no ion temperature increase (see Fig. 14). (2) In the other regime, with an initial density of 3.8×10^{13} cm^{-3} and $T_e(0)$ of 1.2 keV, a temperature rise of 0.5 to 0.6 keV was observed. In this case the efficiency was measured at 90% with the ordinary wave being completely absorbed by the plasma. There was ion heating, with a temperature rise of about 100 eV, but no decrease in density.

In both cases, there was an observable decrease in the energy containment time τ_E. These two regimes were characterized not only by the different densities but also by the wall conditioning. Note that the energy containment time scaling differed from that found earlier on TM-3.[11,12]

Alikaev et al.[30] also made measurements of the electron thermal conductivity in T-10 in the presence of ECH and found that it increased. This increase in κ_e was associated with an increase in T_E and a decrease in τ_E. The experimental value of κ_e rose as much as a factor of 3 with a rise in T_e from 1.5 keV to 2.5 keV but nevertheless remained below the value predicted by scaling laws.

Meanwhile, other experiments were providing new insights. Baranov et al.[31] employed an extraordinary wave launched from the inside of FT-1 with a 29.17-GHz gyrotron (see Fig. 15). With a 2 ms pulse of 60-80 kW, clear bulk heating was observed. The inside antenna was found to be about three times more effective than an outside antenna. The absorption efficiency was about 60%. Further studies in FT-1 by Bulyginsky[32] observed heating above the critical density n_c. Densities up to 2.4 n_c were employed with the heating efficiency remaining unchanged. However, the zone of temperature rise moved outward to the plasma periphery as the density increased.

In a later analysis of these experiments,[33] it was shown that ECH caused a decrease in τ_E. The explanation given was that the heating zone was displaced outward toward the plasma periphery as compared to ohmic heating. There may also have been some increase in κ_e. This analysis involved ray tracing and energy deposition calculations that indicated reductions in τ_E for all cases studied but particularly large reductions for high density. The problem was ascribed to the particular antenna pattern used, which allowed much of the radiation to reach the cyclotron resonance near the periphery without transiting the plasma center. It was speculated that a more directed antenna pattern might have allowing τ_E to increase.

On TM-4,[34] a new gyrotron was used to produce 150 kW for 6 ms at a wavelength of 3.6 mm (~85 GHz). Only second harmonic ECH was employed, with a toroidal magnetic field of ~14 kG. Again, a large electron temperature rise was observed, with $T_e(0)$ increasing from ~700 eV to ~1800 eV but with a density decrease of 25-30%. The new feature of this experiment was the presence of a Cs^+ beam for plasma potential measurements. No observable potential change in the plasma core was detected due to ECH but a slight increase in potential in the periphery was observed. It was thought that the peripheral plasma potential change might be responsible for the change in the global particle balance and hence the density drop.

Contemporary Experiments

Preliminary results from Doublet III (DIII)[35] with outside launch of ordinary mode radiation at 60 GHz are encouraging. Up to 255 kW of power has been delivered to the plasma with a central resonant field of 21.4 kG. Electron temperature increases of 1 keV at the center have been observed by Thomson scattering. A density range of 2-3 × 10^{13} cm^{-3} is used. Profile broadening with off-axis heating has been observed. There is evidence of ion heating. At present only two 60 GHz gyrotrons are in place. Eventually, ten gyrotrons will be available, and inside extraordinary launch will also be attempted. The experimental arrangement and the waveguide system have been described in detail by Moeller[36] (see Fig. 16).

In the Poloidal Divertor Experiment (PDX),[37] a similar system has been prepared. Up to 400 kW of power from two 60-GHz gyrotrons is supplied to the plasma. A novel system of waveguides using the hybrid waveguide mode HE_{11} is used to control the polarization. The HE_{11} mode provides very uniform polarization and no cross-polarization. The system has been described in detail by Doane[38] (see Figs 17 and 18). The first phase of this experiment has been completed and the PDX device has been shut down. Heating has been observed, but the results have not yet been published.

On ISX-B, a 300 kW, 35 GHz gyrotron from NRL will be used to supply power to a rotatable antenna on the high-field side for current-drive and bulk heating experiments. In this case a TE_{04} gyrotron is used, and the radiation is mode converted to TE_{01} for long-distance transmission to the tokamak.

On WT-II,[39] a 35.5-GHz gyrotron supplying up to 30 kW for 10 ms has supplied power for preionization. The preionization produces a plasma for a lower hybrid current drive system. Currents of up to 4.5 kA have been created without ohmic heating.

There have been reports[40] that a 350-kW, 100-GHz gyrotron with a pulse length of 60 ms was installed on T-10 last year and actually used. However, to date there have been no published reports from the U.S.S.R.

Stellarator Experiments

The magnetic configuration of a stellarator or torsatron is quite different from that of a tokamak. Figure 19 shows a possible configuration (in this case Heliotron-E) with the electron cyclotron resonance, UH resonance, and cutoff zones noted. For this particular case, the waveguide launches the microwave power from the low-field side so that only the ordinary mode can propagate directly to the resonance. However, the extraordinary mode is refracted by the plasma,

and reflected from the walls, and it can reach the resonances through multiple scattering around the edge of the plasma.

An early experiment on the Wendelstein IIb stellarator[41] used ECH to produce very weakly ionized plasmas. A density of $\approx 1 \times 10^{12}$ cm^{-3} was produced with ≈1 W of rf heating at a frequency of 9.2 GHz. The temperature was about 10 eV. In the Saturn stellarator,[42] experiments using 10-GHz power produced plasmas with low electron temperatures. With <15 W of power, a temperature of 8-10 eV was achieved with a plasma density of $1\text{-}2 \times 10^{11}$ cm^{-3}; with ≈600 W of power, a temperature of 20 eV and a density of 2×10^{12} cm^{-3} were reached.

In the CLEO stellarator,[43] 12 kW of power at 17.5 GHz created a plasma density of $1.5\text{-}2.5 \times 10^{12}$ cm^{-3} with $T_e \approx 50\text{-}100$ eV for 50-100-ms pulses. In this case the critical density was 4×10^{12}, cm^{-3}, so a plasma of about half the critical density was created.

In the JIPPT-2 stellarator,[44] a plasma was created with 13 kW of 35.5-GHz power. A density of 2×10^{12} cm^{-3} was achieved, about 20% of the cutoff density. This plasma was used for effective preionization in ohmic discharges. Power levels up to 40 kW were also used to heat the ohmic plasma in this stellarator. A heating efficiency independent of the mode (O- or X-mode) was found, and this was interpreted to mean that the X-mode power (which should have been cut off by the launching technique) scattered around the plasma periphery to reach the resonance

zones. The absorption efficiency was about 0.5 at a plasma density of 6×10^{12} cm^{-3}.

A 28-GHz gyrotron was used on the Heliotron-E experiment[45] to produce a plasma with a density of 5×10^{12} cm^{-3} and $T_e \sim 1100$ eV (see Fig 20). About 90 kW of power was injected from the low-field side. Ion heating was also observed, with ion temperature T_i reaching 120 eV. An electron heating efficiency of 10 eV/kW was found, which is about twice that observed for tokamaks.[14] In both the CLEO and Heliotron-E experiments the containment time for the ECH-created plasmas was better than for ohmic plasmas (Fig 21). The interpretation is that in both cases the drift parameter ξ ($\xi = v_d/v_{th}$, where v_d is the electron drift velocity and v_{th}, is the electron thermal velocity) is much smaller for this kind of plasma since no toroidal electric field is needed.

Future Experiments

Plans include the possibility of large amounts of power for the T-15 tokamak at the Kurchatov Institute. Several megawatts of 100 GHz power are planned for this experiment.[40] For the Wendelstein VIIa experiment in Garching, both 28- and 60-GHz power will be used.[46] Only one 28 GHz gyrotron will be used but up to four 60-GHz gyrotrons are envisaged. Careful mode control and launching angle and polarization are planned (see Fig 22). On the Advanced Toroidal Facility (ATF-1), preionization and target plasma production with 35 GHz and 53 GHz gyrotrons are planned. On Heliotron-E 53.2 GHz gyrotrons will be used

to increase the plasma density.[47] At Culham, additional power at 28 GHz and 60 GHz is planned for CLEO, DITE, and COMPASS.[48]

For the International Tokamak Reactor (INTOR) experiment, Alikaev[49] has suggested the use of 5 MW of 100 GHz power from a gyrotron complex of twenty-four 200 kW gyrotrons. Lashmore-Davies and Riviere[50] have discussed the use of massive ECH for startup in the INTOR plasma. There are calculations[51] suggesting that for very large tokamaks outside O-mode launch would be preferable. This is due to the strong surface heating of the X-mode from the inside, the difficulty of launching from the inside, and, finally, the strong central heating of the outside O-mode launch.

Summary

This paper has reviewed early ECH experiments with small amounts of ECH power and small devices. The early success led to advanced designs. In the United States, England, and Japan, tokamak and stellarator results have shown bulk heating, profile modification, and possible current drive. There is evidence that the outside O-mode launch is much less effective than inside X-mode launch in present-day experiments. However, one stellarator experiment showed that O- and X-mode power were equally well absorbed. The evidence for current drive is not strong and does not permit confident predictions for large devices. Experiments at the megawatts level will begin soon, and a promising future appears to be at hand. Careful mode control and power handling are planned for these new experiments, as are detailed studies of ray tracing and power deposition.

References

1. W. B. Ard et al., Bull. Am. Phys. Soc. 5(6), 189 (1960); M. C. Becker et al., p. 345 in Proceedings of the International Conference on Plasma Physics and Controlled Nuclear Fusion Research, Vol. 1, International Atomic Energy Agency, Vienna, 1962.

2. J. Schneider, Phys. Rev. Lett. 2, 504 (1959); J. L. Hirshfield and J. M. Wachtell, Phys. Rev. Lett. 12, 533 (1959); A. V. Gaponov, Izv. Vyssh. Uchebn. Zaved. Radiofiz. 2, 836 (1959).

3. N. I. Zaytsev et al., Radiotekh. Elektron. [Radio Eng. Electron. (U.S.S.R.)] 19, 103 (1974).

4. V. E. Golant et al., Sov. Phys.-Tech. Phys. 17, 488 (1972).

5. V. E. Golant and A. D. Piliya, Usp. Fiz. Nauk (Sov. Phys.-Usp.) 14, 413 (1972).

6. V. V. Alikaev et al., p. 108 in Proceedings of the 5th European Conference on Controlled Nuclear Fusion and Plasma Physics, Vol. 1, Grenoble, France, 1972.

7. V. V. Alikaev et al., JETP Lett. 15, 27 (1972).

8. V. E. Golant et al., paper E5 in Proceedings of the 3rd International Symposium on Toroidal Plasma Confinement, Garching, Federal Republic of Germany, 1973.

9. V. E. Golant et al., p. 587 in Proceedings of the 6th European Conference on Controlled Nuclear Fusion and Plasma Physics, Vol. 1, Moscow, 1973.

10. V. V. Alikaev et al., p. 241 in Plasma Physics and Controlled Nuclear Fusion Research: Proceedings of the 5th International Conference, Vol. 1, International Atomic Energy Agency, Vienna, 1974.

11. V. V. Alikaev et al., Sov. J. Plasma Phys. 2, 212 (1976).

12. V. V. Alikaev et al., p. 144 in Proceedings of the 7th European Conference on Controlled Nuclear Fusion and Plasma Physics, Vol. 1, 1975.

13. V. I. Pozynak, Sov. J. Plasma Phys. 7, 445 (1981).

14. R. M. Gilgenbach et al., Phys. Rev. Lett. 44, 647 (1980).

15. R. M. Gilgenbach et al., Nucl. Fusion 21, 319 (1981).

16. M. W. Alcock et al., papers H-1 and H-15 in Proceedings of the 10th European Conference on Controlled Fusion and Plasma Physics, Moscow, 1981.

17. D. C. Robinson et al., paper E-3 in Heating in Toroidal Plasmas: Proceedings of the 3rd Joint Varenna-Grenoble International Symposium, Grenoble, 1982.

18. M. W. Alcock et al., paper IAEA-CN-41/I-5 in Plasma Physics and Controlled Nuclear Fusion Research: Proceedings of the 10th International Conference, Baltimore, September 1-8, 1982, International Atomic Energy Agency, Vienna (in press).

19. D. F. Start et al., paper H-16 in Proceedings of the 10th European Conference on Controlled Fusion and Plasma Physics, Moscow, 1981; D. F. Start et al., Phys. Rev. Lett. 48, 624 (1982).

20. R. J. LaHaye et al., Nucl. Fusion 21, 1425 (1981).

21. C. P. Moeller et al., Phys. Fluids 25, 1211 (1982).

22. J. S. Levine et al., in Proceedings of the 3rd International Conference on ECH and ECE in Plasmas, Madison, 1982 (in press).

23. F. S. McDermott et al., Phys. Fluids 25, 1488 (1982).

24. Y. Terumichi et al., p. 135 in Proceedings of Workshop on High Power Heating, Kyoto, Japan, 1980

25. Y. Terumichi et al., paper D3 in Proceedings of the 4th Topical Conference on RF Heating in Plasmas, Univ. Texas, Austin, 1980.

26. V. S. Strehlkov, p. 387 in Proceedings of the 9th European Conference on Controlled Fusion and Plasma Physics: Invited Papers, Oxford, 1979.

27. V. V. Alikaev et al., p. 1 in Proceedings of the 10th European Conference on Controlled Fusion and Plasma Physics: Invited Papers, Moscow, 1981; V. V. Alikaev, paper H-3 in Proceedings of the 10th European Conference on Controlled Fusion and Plasma Physics, Vol. 1., Moscow, 1983.

28. V. A. Flyagin et al., p. 1059 in Heating in Toroidal Plasmas: Proceedings of the 3rd Joint Varenna-Grenoble International Conference, Vol. III, 1982.

29. V. V. Alikaev et al., JETP Lett. 35, 140 (1982).

30. V. V. Alikaev et al., JETP Lett. 35, 163 (1982).

31. Yu. F. Baranov et al., paper H-8 in Proceedings of the 10th European Conference on Controlled Fusion and Plasma Physics, Vol. 1., Moscow, 1983.

32. D. G. Bulyginsky et al., p. 561 in
Proceedings of the 10th European Conference on
Controlled Fusion and Plasma Physics, Supplement, Moscow, 1983.

33. Yu. F. Baranov et al., paper IAEA-CN-41/J4 in Plasma Physics and
Controlled Nuclear Fusion Research: Proceedings of the 10th International
Conference, Baltimore, September 1-8, 1982, International Atomic Energy
Agency, Vienna (in press).

34. A. V. Gorshkov et al., p. 571 in
Proceedings of the 10th European Conference on
Controlled Fusion and Plasma Physics, Supplement, Moscow, 1983.

35. R. Prater et al., in
Proceedings of the 5th Topical Conference on RF Heating in Plasmas, Madison,
1983 (in press).

36. C. P. Moeller, p. 1085 in Heating in Toroidal Plasmas:
Proceedings of the 3rd Joint Varenna-Grenoble International Conference,
Vol. III, 1982; and C. P. Moeller et al., in
Proceedings of the 5th Topical Conference on RF Heating in Plasmas, Madison,
1983 (in press).

37. H. Hsuan, Bull. Am. Phys. Soc. 27, 1049 (1982).

38. J. Doane, Int. J. Electron. 53(6), 573 (1983).

39. Y. Terumichi, in Proceedings of the 5th Topical Conference on RF
Heating in Plasmas, Madison, 1983 (in press).

40. A. Cavallo, University of Maryland, private communication.

41. R. Ellis and D. Eckart, Max Planck Institute for Plasma Physics
report IPP2/85, Garching, Federal Republic of Germany (1970).

42. V. L. Berezhnyy et al., Kharkov Physical-Technical Institute report KHFTI-74-42, Kharkov, U.S.S.R. (1974).

43. D. W. Atkinson et al., p. 153 in Plasma Physics and Controlled Nuclear Fusion Research: Proceedings of the 8th International Conference, Vol. 1, International Atomic Energy Agency, Vienna, 1981.

44. K. Ohkubo et al., Nucl. Fusion 22, 1085 (1982); K. Ohkubo et al., Nucl. Fusion 21, 1320 (1981); T. Amano, paper IAEA-CN-41/C3 in Plasma Physics and Controlled Nuclear Fusion Research: Proceedings of the 10th International Conference, Baltimore, September 1-8, 1982, International Atomic Energy Agency, Vienna (in press).

45. K. Uo et al., paper IAEA-CN-41/L3 in Plasma Physics and Controlled Nuclear Fusion Research: Proceedings of the 10th International Conference, Baltimore, September 1-8, 1982, International Atomic Energy Agency, Vienna (in press); K. Uo et al., p. 1091 in Heating in Toroidal Plasmas: Proceedings of the 3rd Joint Varenna-Grenoble International Conference, Vol. III, 1982.

46. V. Erckmann et al., paper C-3.2 in Proceedings of the 5th Topical Conference on RF Heating in Plasmas, Madison, 1983 (in press).

47. K. Uo, Heliotron Laboratory, private communication.

48. W. H. M. Clark et al., Culham Laboratory report CLM-R225, Culham, England (1982).

49. V. V. Alikaev, I. V. Kurchatov Institute of Atomic Energy, private communication.

50. C. N. Lashmore-Davies and A. C. Riviere, p. 1079 in
Heating in Toroidal Plasmas:
Proceedings of the 3rd Joint Varenna-Grenoble International Conference,
Vol. III, 1982.

51. A. G. Litvak et al., Nucl. Fusion 17, 659 (1977).

Figure Captions

Fig. 1. CMA diagram.

Fig. 2. Typical tokamak with (a) low-density plasma, (b) moderate-density plasma, and (c) high-density plasma.

Fig. 3. Experimental arrangement in FT-1 (from Golant et al., Ref. 8).

Fig. 4. Temporal dependence of laser temperature rise in TM-3 (from Alikaev et al., Ref. 12).

Fig. 5. Dependence of average energy containment time τ_E on average electron temperature (-o--o-) and of energy confinement time for central column region on the maximum electron temperature (-x--x-) (from Alikaev et al, Ref. 12).

Fig. 6. Experimental configuration. The electron cyclotron frequency (f_c) is shown for a toroidal magnetic field B_t of 12.5 kG on axis (from Gilgenbach et al., Ref. 14).

Fig. 7. (a) Electron temperature profile and (b) density profile measured by Thomson scattering. Dashed lines denote data taken before ECH (118 ms into tokamak shot); solid lines represent data at the end of ECH (130 ms). Data are for 80-kW microwave injection with a 10-ms ECH pulse starting at 120 ms, B_t = 12.5 kG, line-averaged electron density $n_e \sim 10^{13}$ cm^{-3}, and plasma current I_p = 83 kA (from Gilgenbach et al., Ref. 14).

Fig. 8. X-ray emission profile showing asymmetric heating (from Alcock et al, Ref. 18).

Fig. 9. Microwave system schematic for the JFT-2 outside launch. The 16° half-power width of a single horn is shown (from LaHaye et al., Ref. 20).

Fig. 10. Schematic diagram of microwave system for the inside launch on JFT-2 (from Moeller et al., Ref. 21).

Fig. 11. Central heating as a function of density measured during the heating pulse for the oblique launch of the X-mode for a central toroidal field of 0.9 T (from Moeller et al., Ref. 21).

Fig. 12. The rf transmission system for VERSATOR II. (a) The overall view. (b) Detail of the antenna (from Levine et al., Ref. 22).

Fig. 13. Layout of the gyrotron complex on T-10. (1) T-10 tokamak. (2) Oversize waveguide. (3) Gyrotron. (4) Cryomagnetic system (5) Quasioplical mitre bends. (6) Electrical break (from Flyagin et al., Ref. 28).

Fig. 14. Radial profiles of the electron temperature and density (1) before and (2) at the end of the heating pulse in T-10 for case 1 (from Alikaev et al., Ref. 29).

Fig. 15. Schematic view of the antenna on FT-1 (from Baranov et al., Ref. 31).

Fig. 16. Schematic diagram of the 60-GHz microwave system associated with each gyrotron on DIII (from Moeller et al., Ref. 36).

Fig. 17. Electric fields in the HE_{11} mode (from Doane, Ref. 38).

Fig. 18. Radiation pattern for the HE_{11} and TE_{01} waveguide modes (from Doane, Ref. 38).

Fig. 19. Experimental configuration on Heliotron-E, showing (1) resonance surface of f_c = 28 GHz (B = 1 T), (2) right-hand cutoff, (3) UH resonance. Ray tracings of ordinary (O) and

extraordinary (X) modes are indicated by solid lines (from Uo *et al.*, Ref. 45).

Fig. 20. Temporal evolution of the central electron and ion temperatures and the average electron density. The rf power is 90 kW. The line-averaged electron density is 5×10^{12} cm^{-3}. The solid lines indicate electron and ion temperatures calculated on the basis of a simple transport model (from Uo *et al.*, Ref. 45).

Fig. 21. Dependence of the electron energy containment time τ_E on the drift parameter for ECH and ohmic plasmas (from Uo *et al.*, Ref. 45).

Fig. 22. Quasi-optical ECH launching system at 60 GHz for Wendelstein VII-AS (from Erckmann *et al.*, Ref. 46).

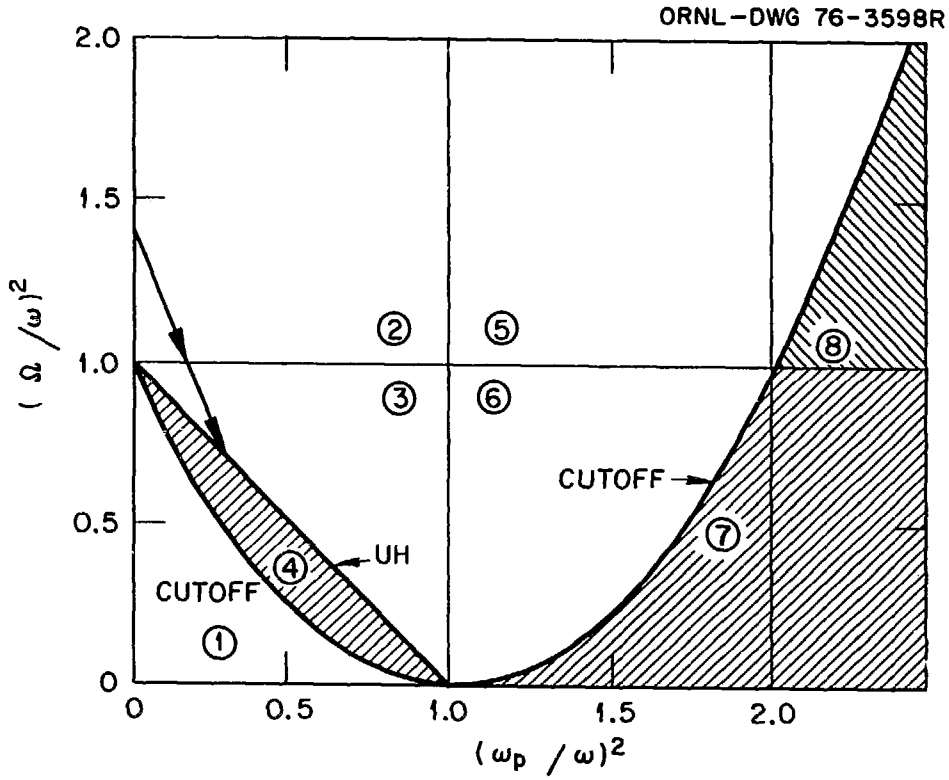
ORNL-DWG 76-3598R
2.0
1.5
1.0
0.5
0
0
0.5
1.0
1.5
2.0
$(\Omega/\omega)^2$
$(\omega_p/\omega)^2$
CUTOFF
UH
CUTOFF
1
2
3
4
5
6
7
8

ORNL-DWG 83-3005 FED

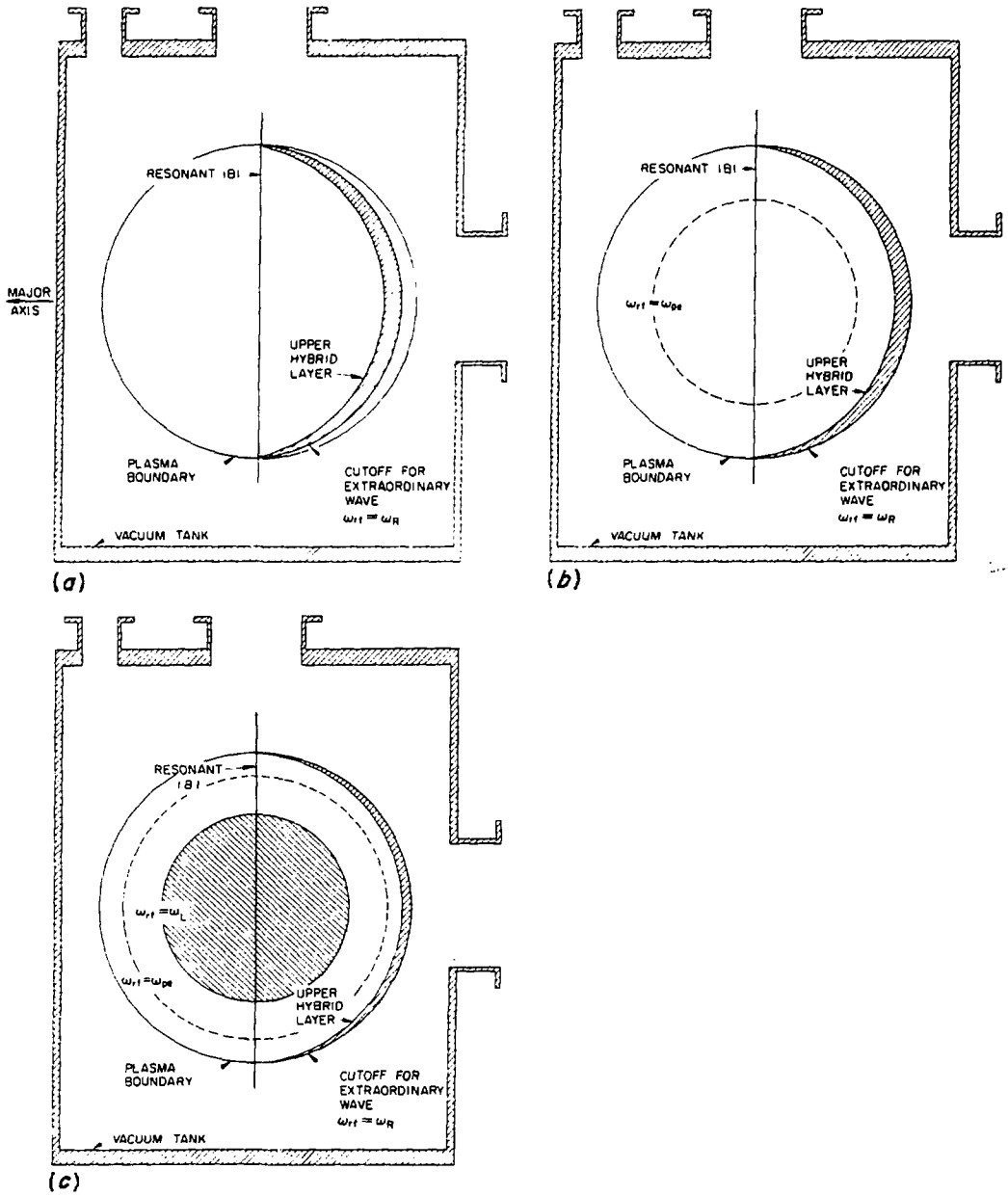

ORNL-DWG 83-3006 FED

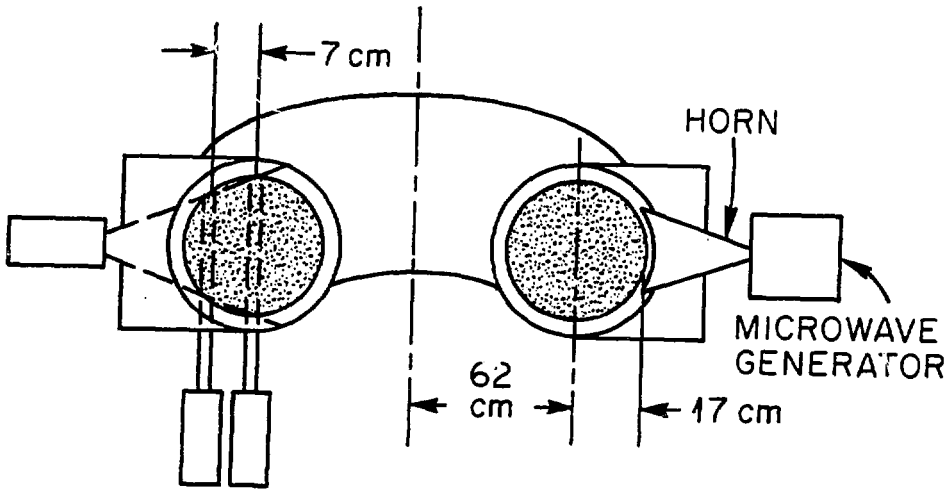

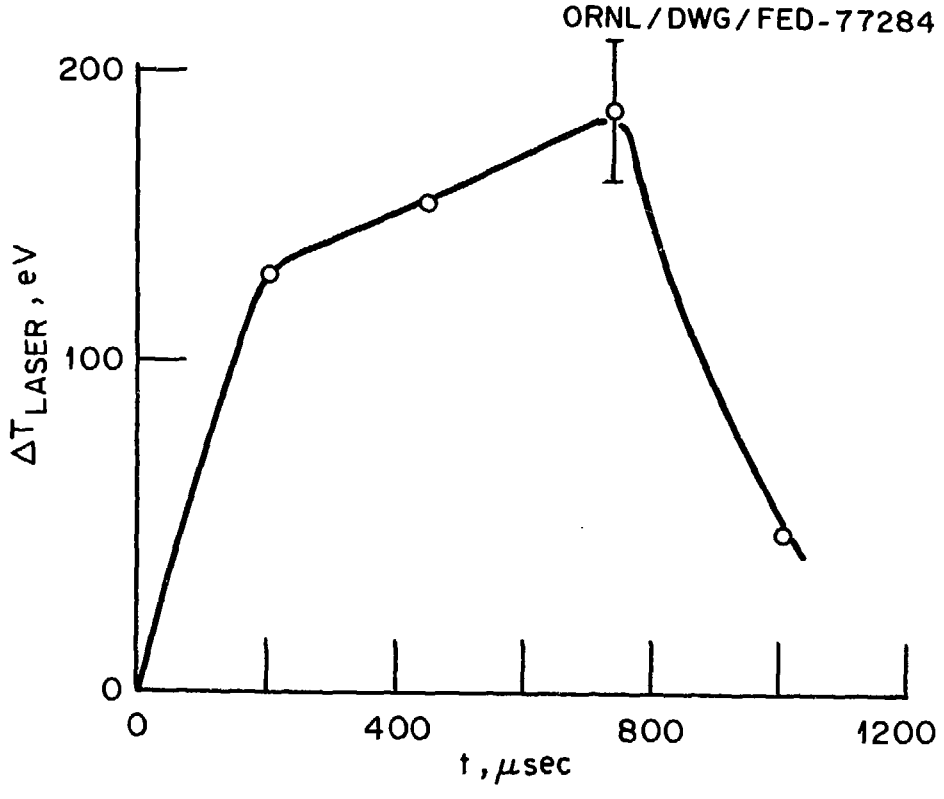
ORNL/DWG/FED-77284
200
100
0
ΔT_{LASER}, eV
0
400
800
1200
t, μsec

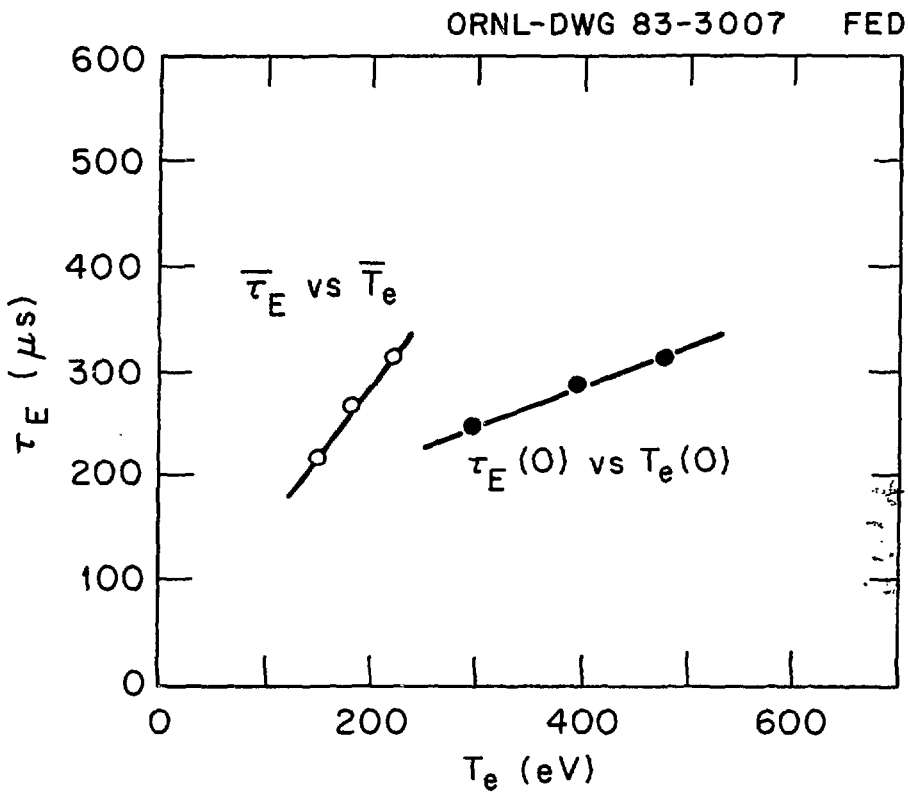
ORNL-DWG 83-3007 FED
600
500
400
300
200
100
0
τ_E (μs)
$\overline{\tau}_E$ vs $\overline{T}_e$
τ_E(0) vs T_e(0)
0
200
400
600
T_e (eV)

ORNL-DWG 80-2135 FED

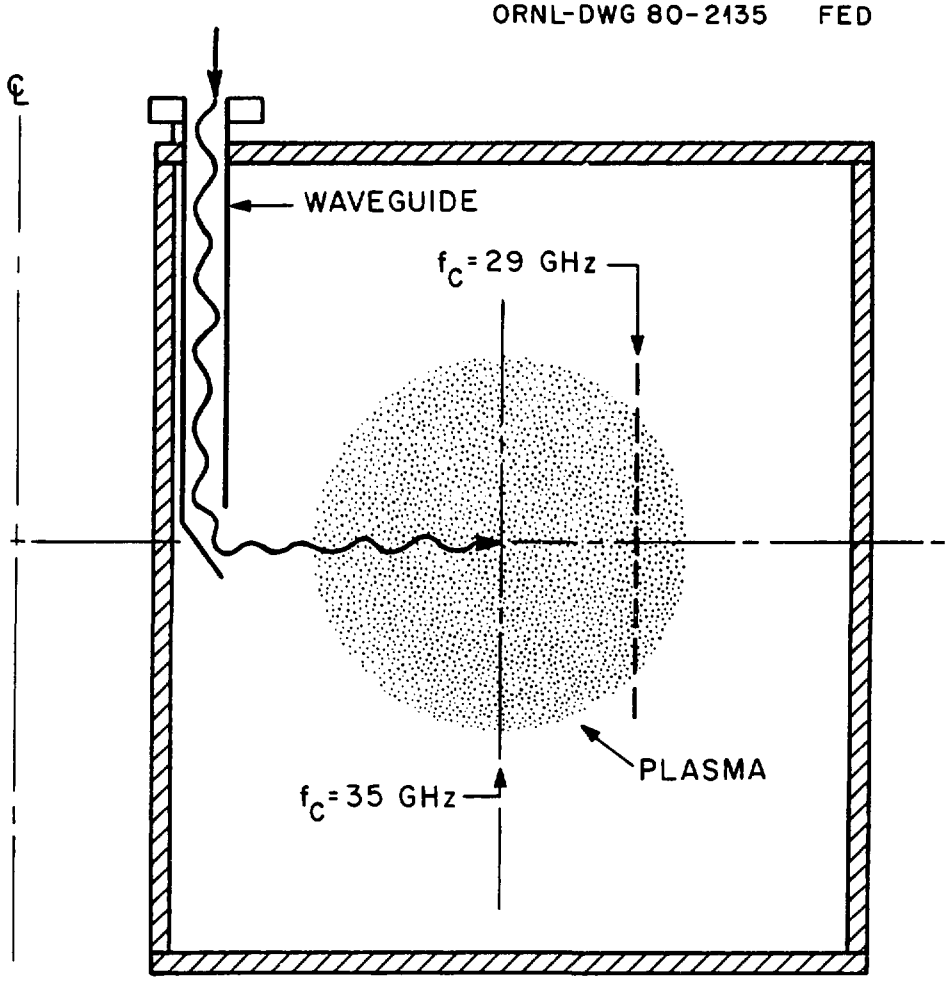

ORNL-DWG 79-3473A FED

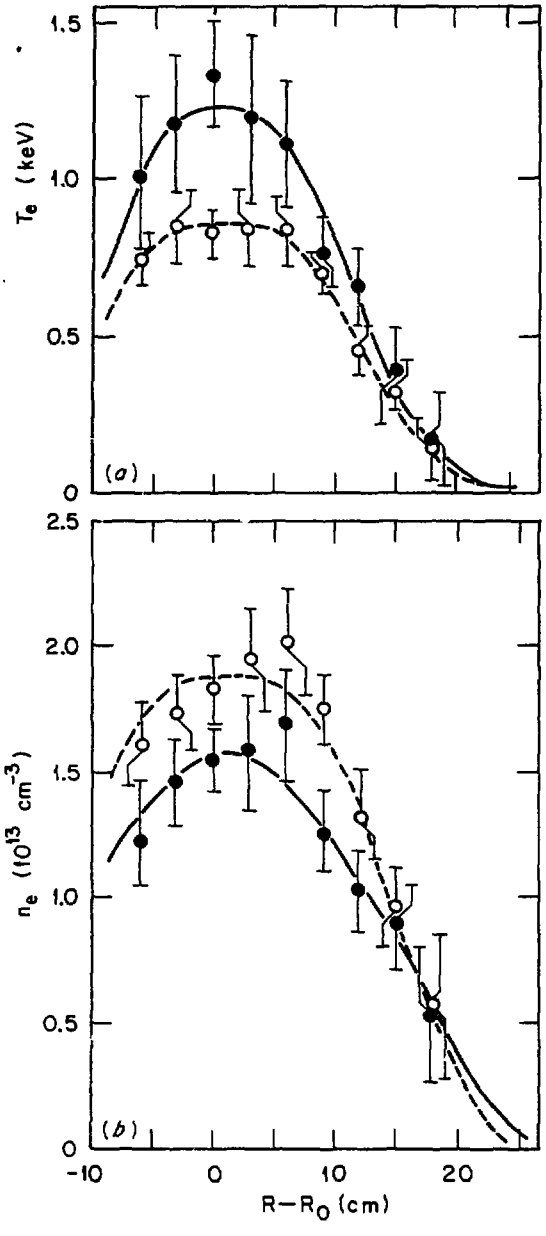

ORNL-DWG 83-3008 FED

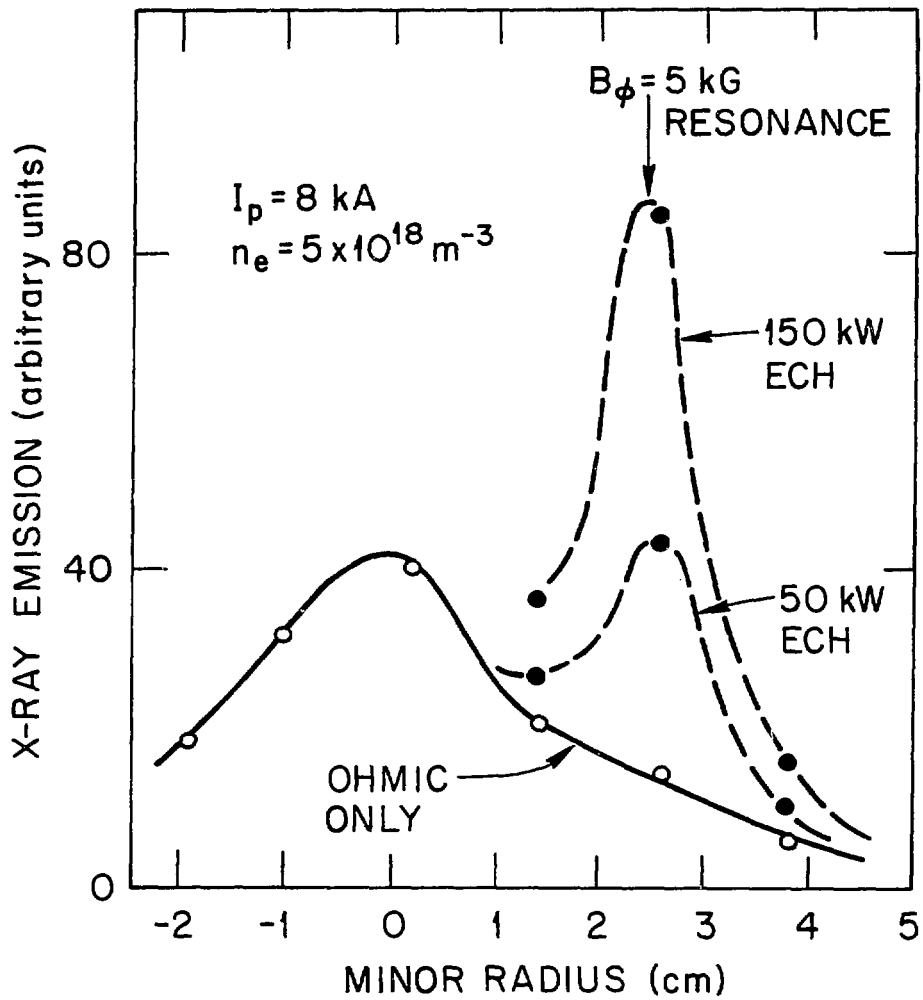

ORNL–DWG 83-3009 FED

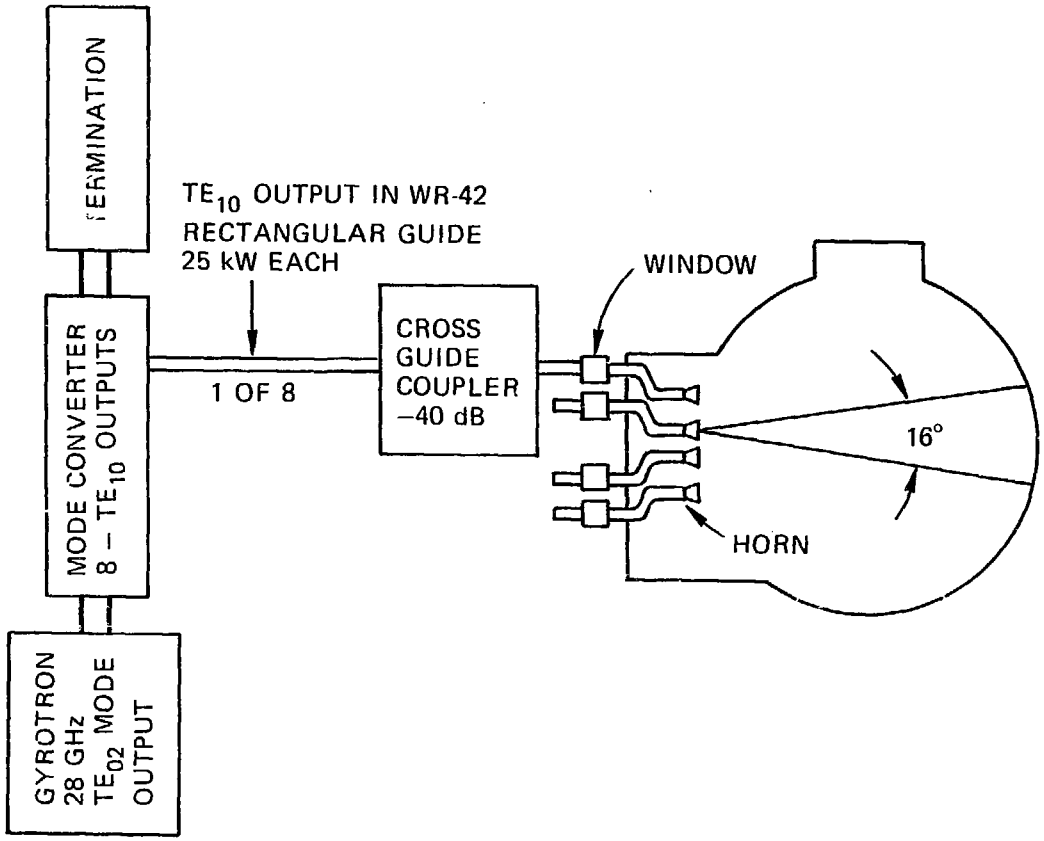

ORNL–DWG 83-3010 FED

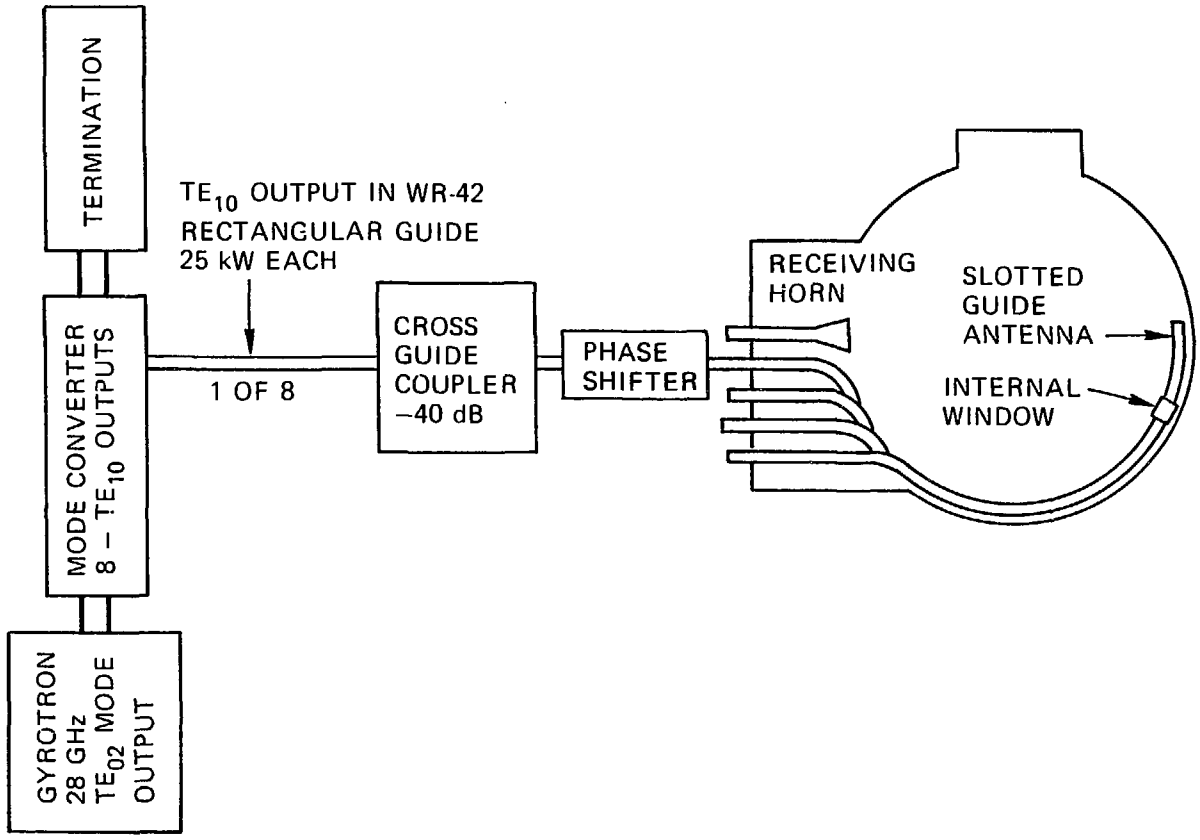

ORNL-DWG 83-3011 FED

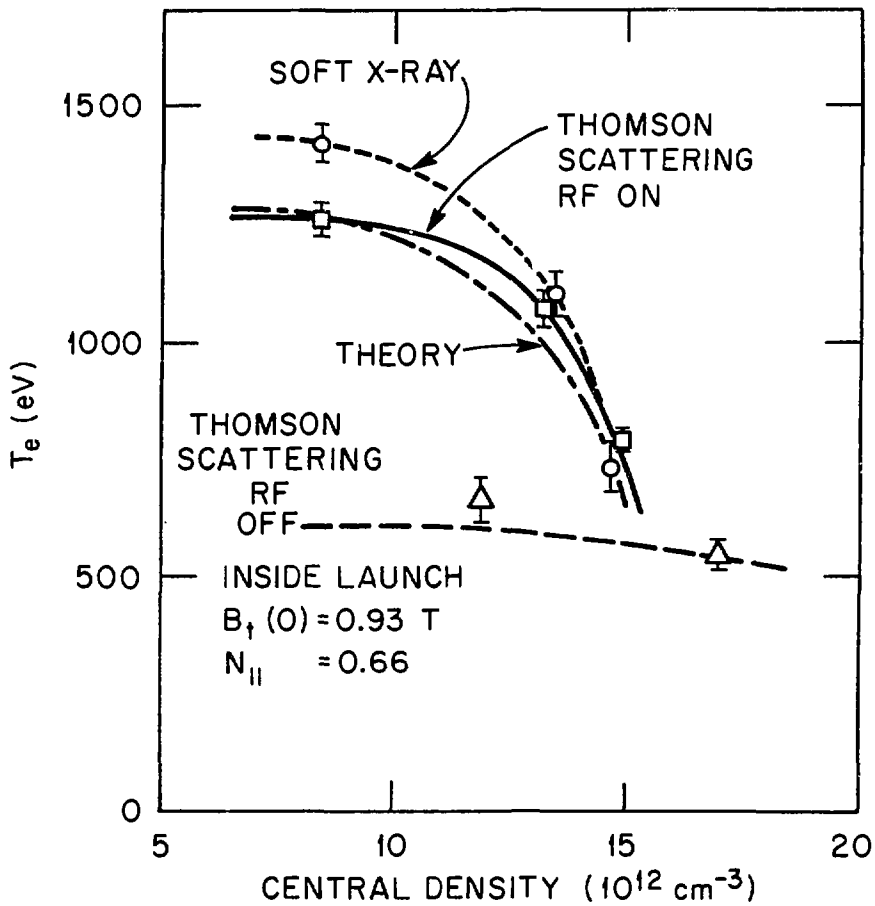

ORNL-DWG 83-3012 FED

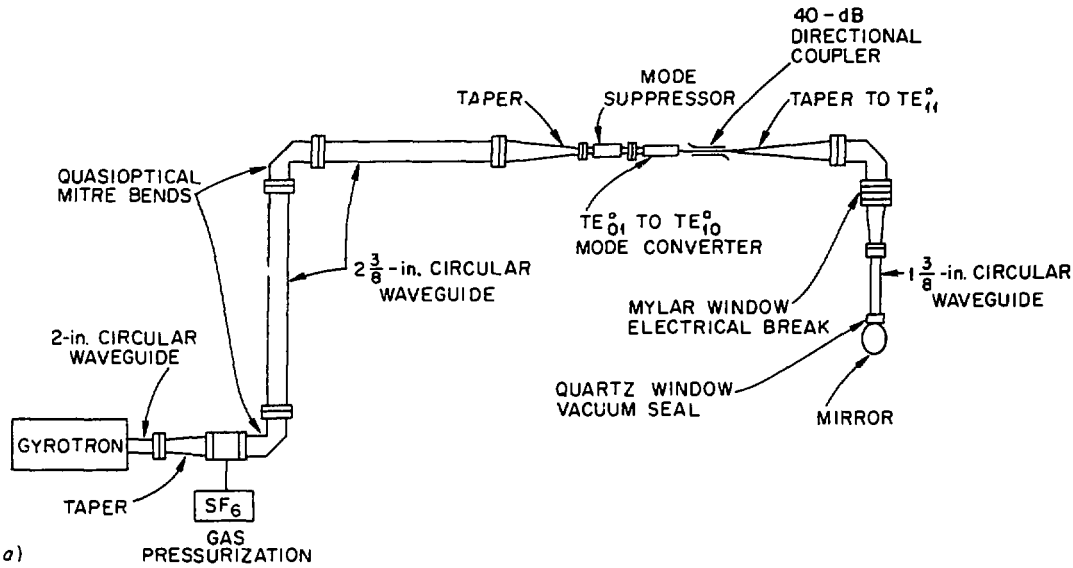

(a)

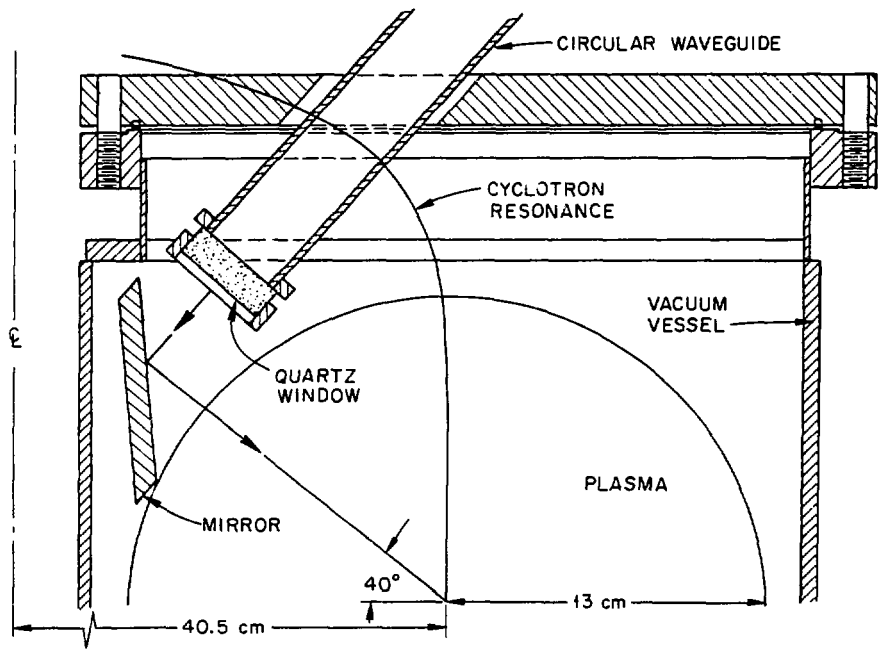

(b)

ORNL–DWG 83-3013 FED

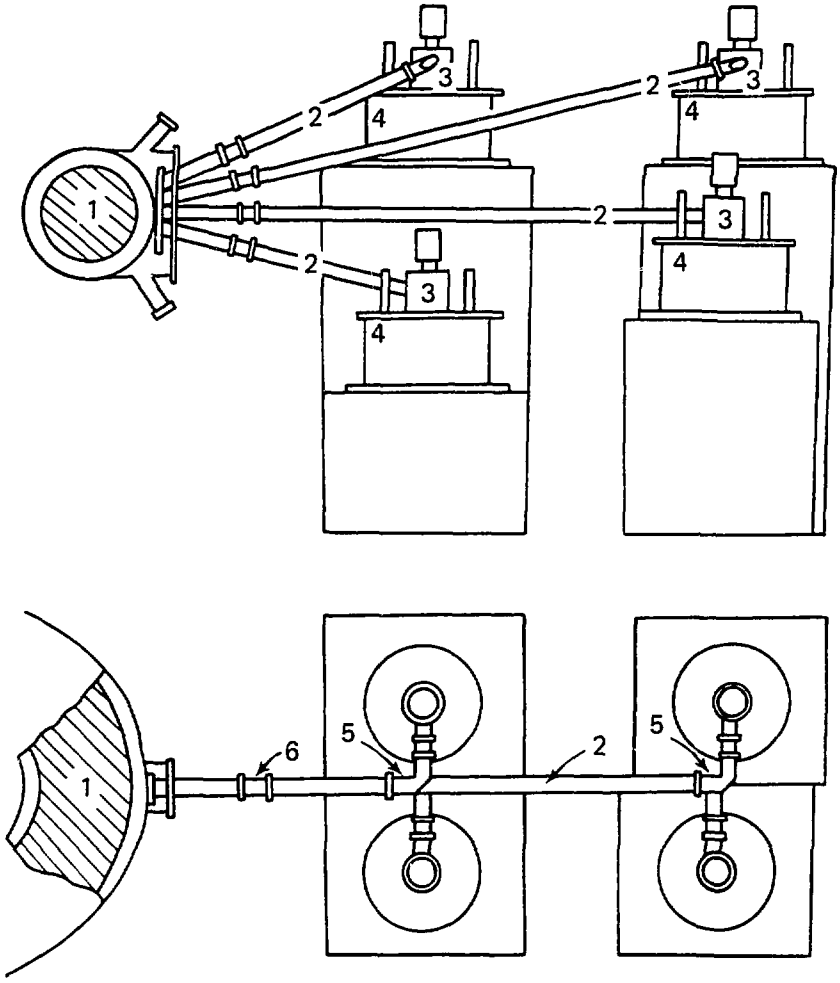

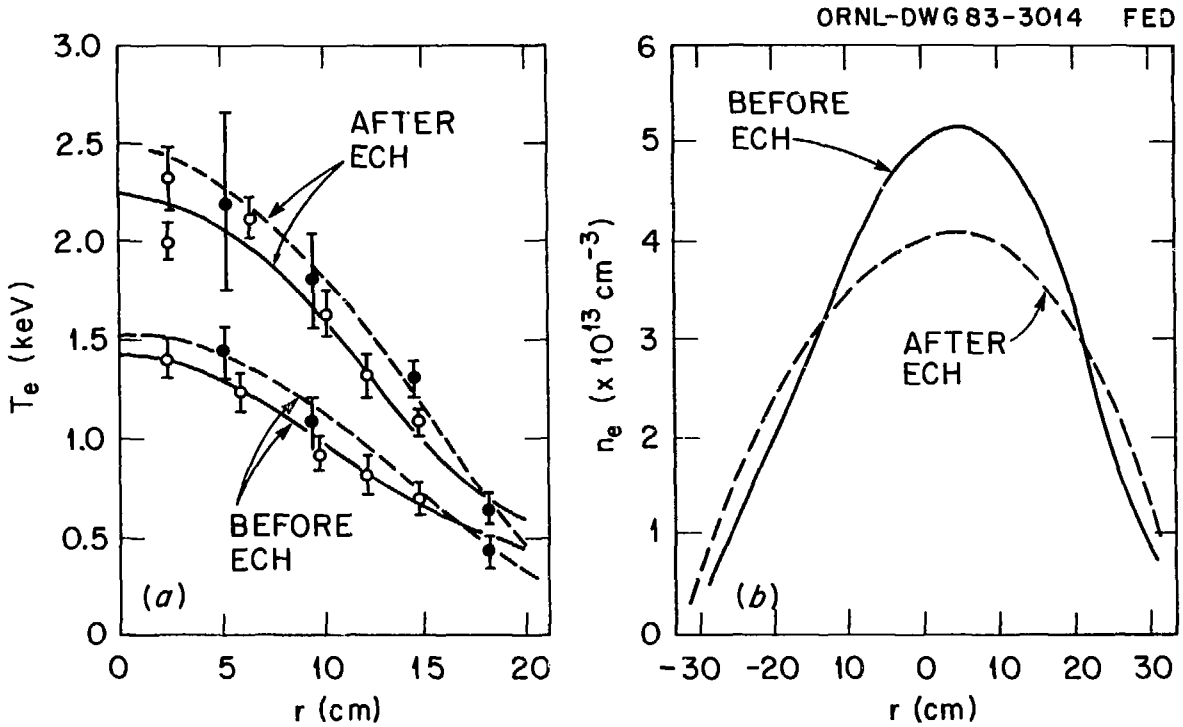
ORNL-DWG 83-3014 FED
3.0
2.5
2.0
1.5
1.0
0.5
0
T_e (keV)
AFTER ECH
BEFORE ECH
(a)
0
5
10
15
20
r (cm)
6
5
4
3
2
1
0
n_e ($\times 10^{13}$ cm^{-3})
BEFORE ECH
AFTER ECH
(b)
-30
-20
10
0
10
20
30
r (cm)

ORNL-DWG 81-2094 FED

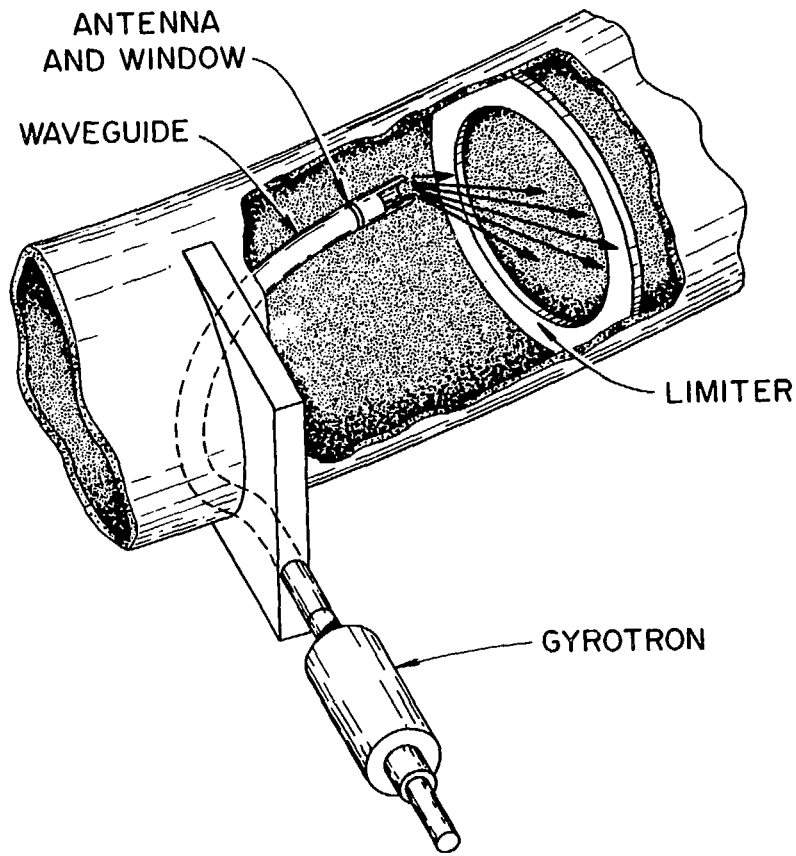

ORNL-DWG 83-3015 FED

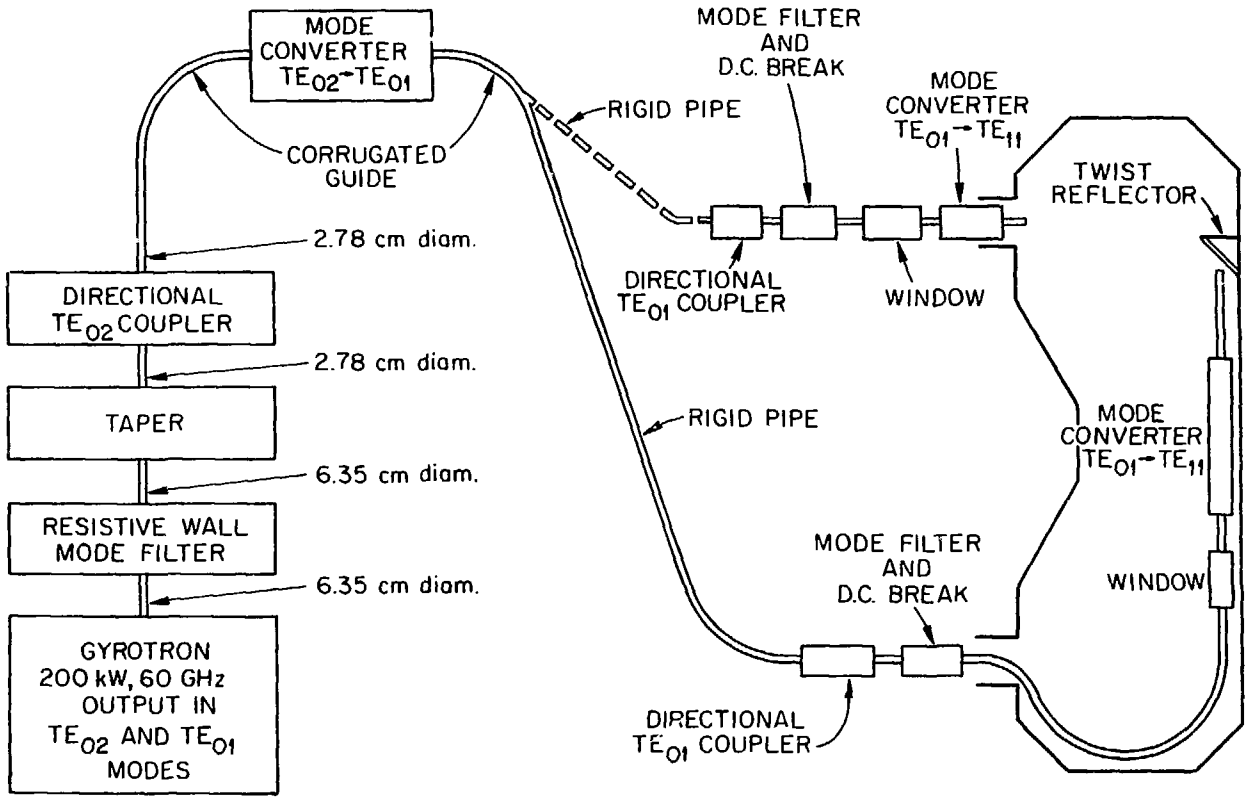

ORNL-DWG 83-3016 FED

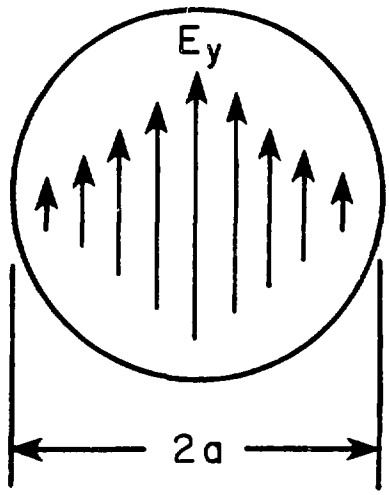

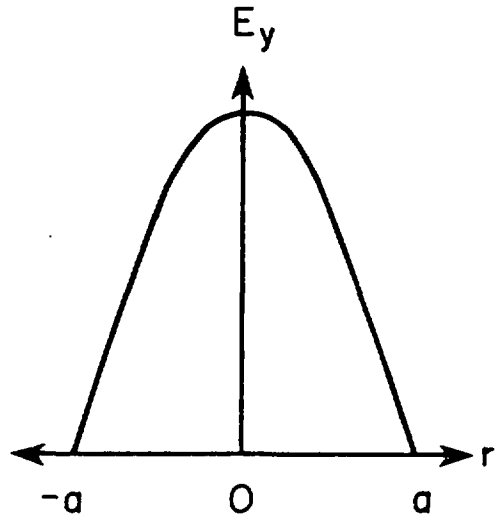

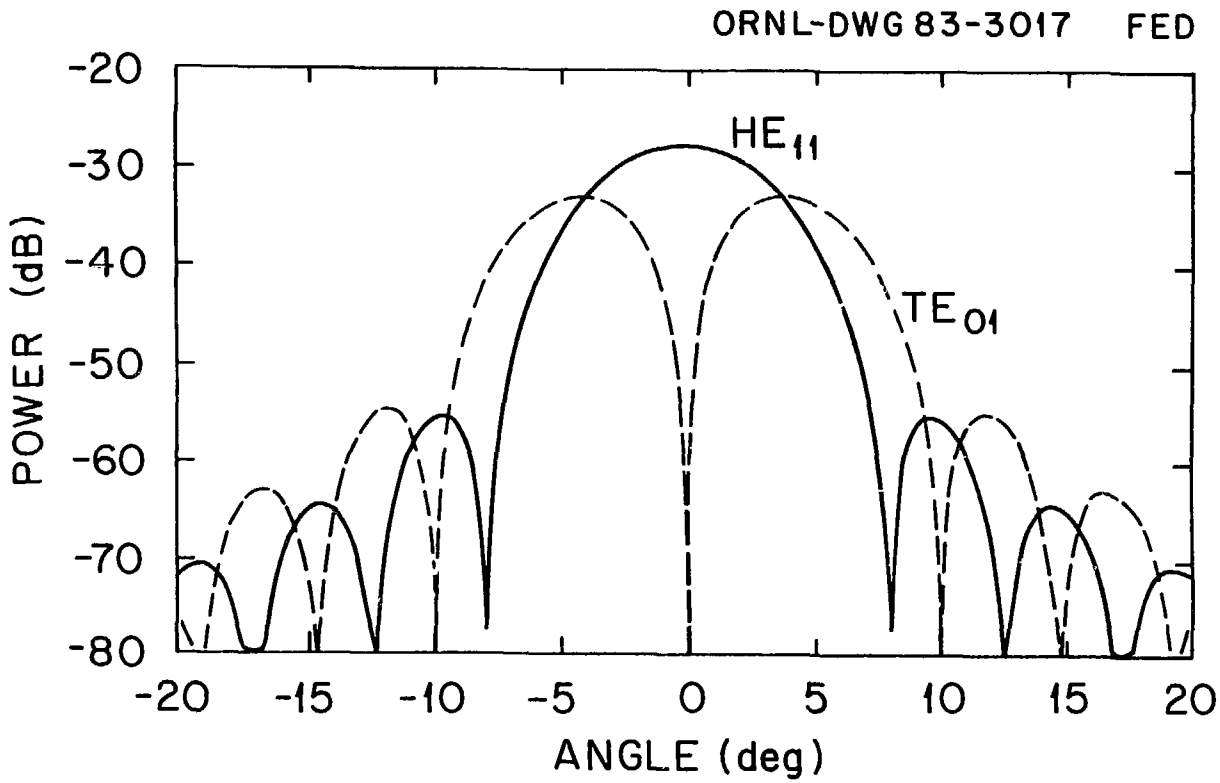
ORNL-DWG 83-3017 FED
HE11
TE01
POWER (dB)
-20
-30
-40
-50
-60
-70
-80
-20
-15
-10
-5
0
5
10
15
20
ANGLE (deg)

ORNL-DWG 83-3018 FED

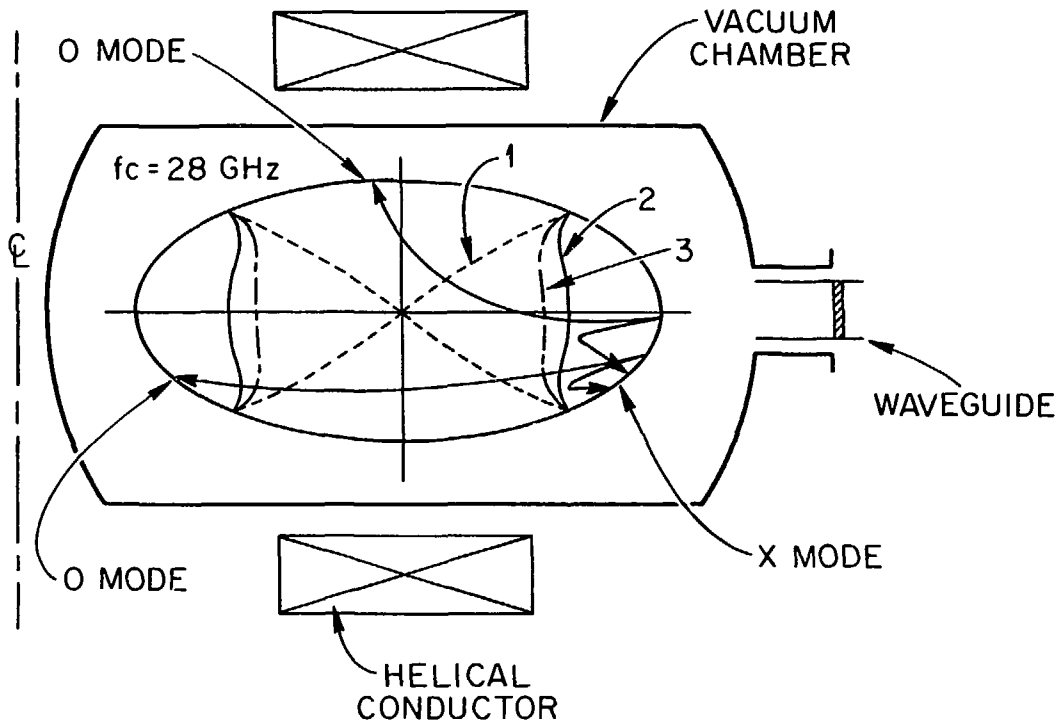

ORNL-DWG 83-3019 FED

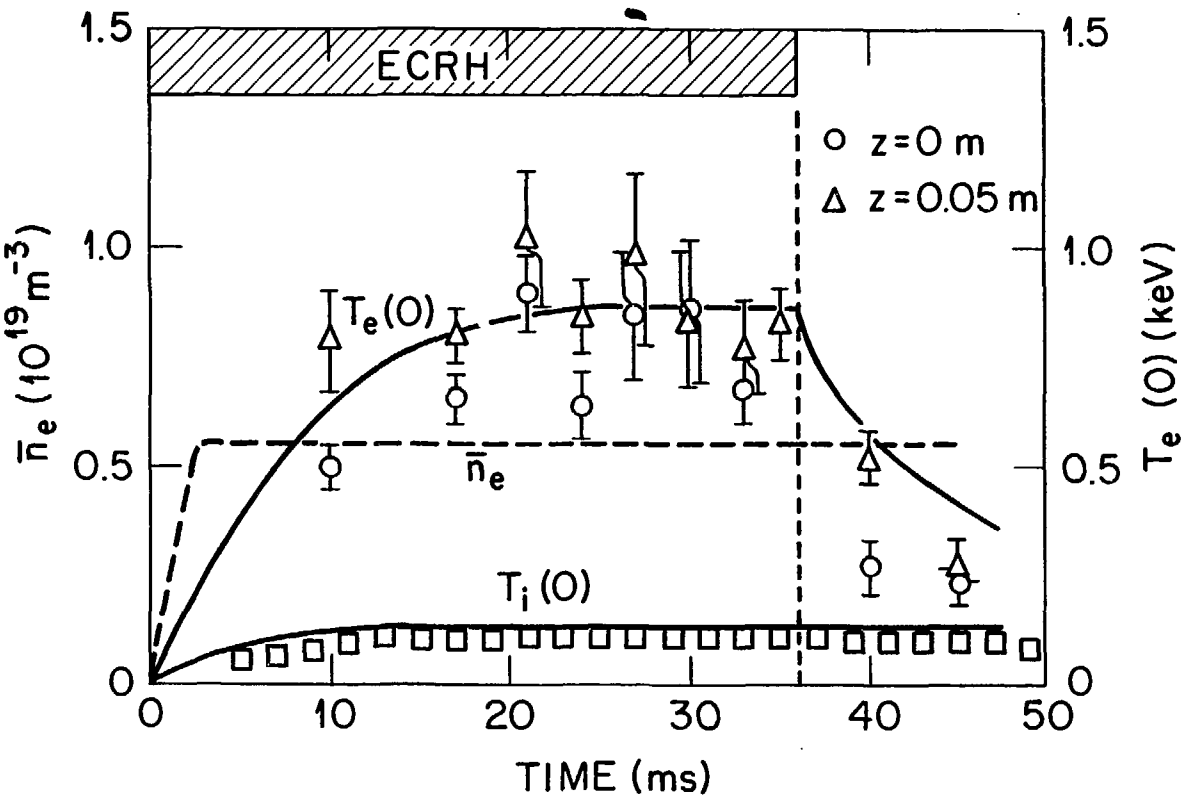

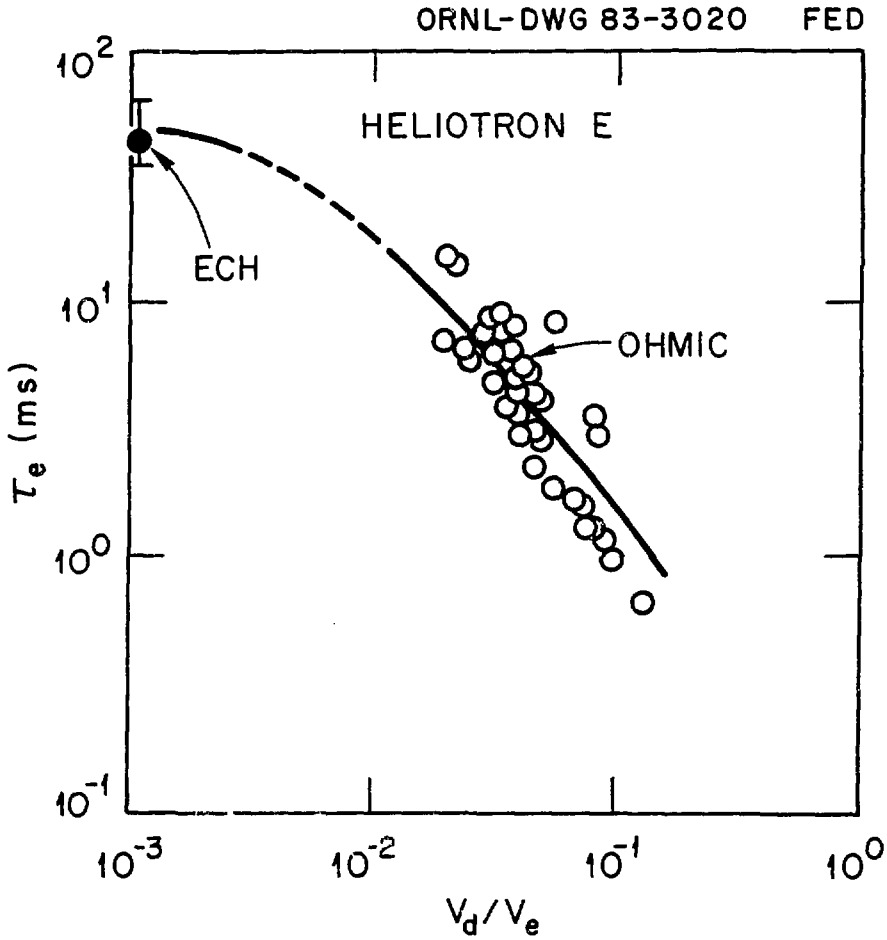
ORNL-DWG 83-3020 FED
HELIOTRON E
ECH
OHMIC
10^2
10^1
10^0
10^{-1}
τ_e (ms)
10^{-3}
10^{-2}
10^{-1}
10^0
V_d/V_e
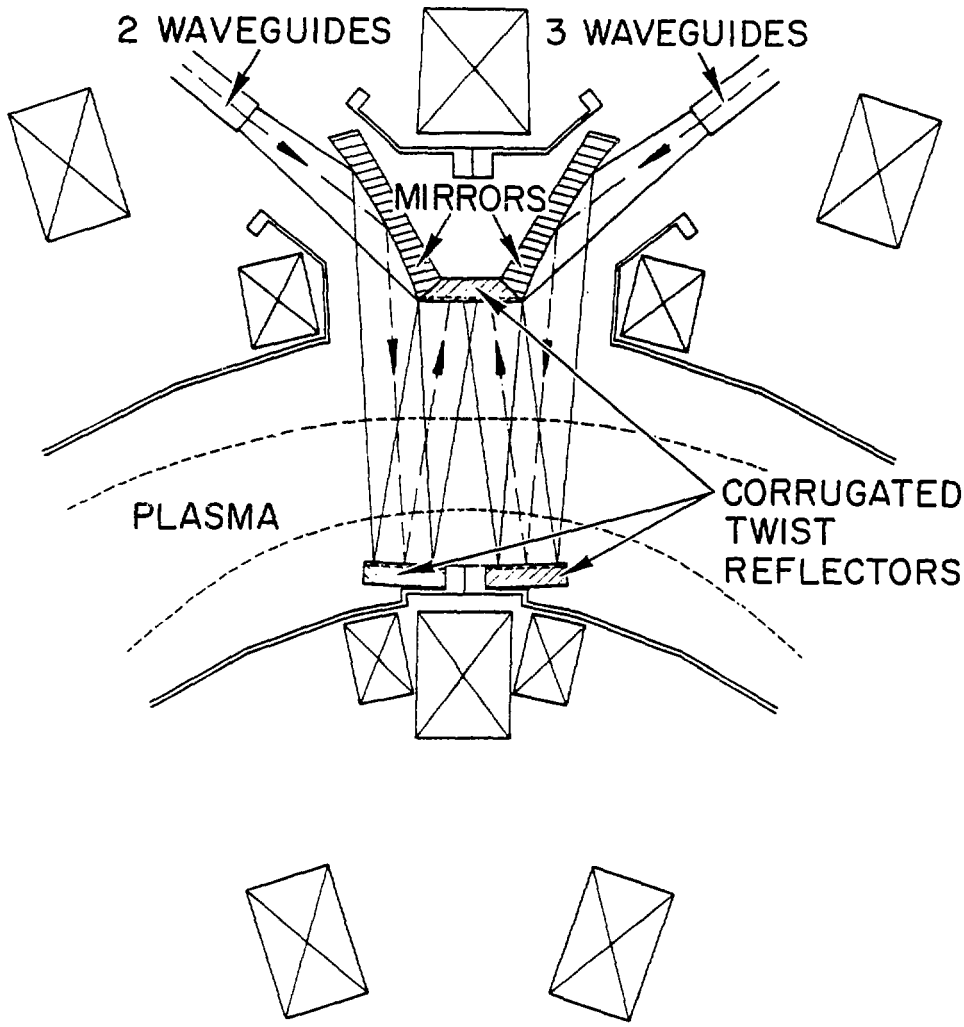
ORNL-DWG 83-3021 FED